

MASS MEASUREMENTS OF EXOTIC LIGHT NUCLEI*

W. Benenson, E. Kashy, D. Mueller and H. Nann
Cyclotron Laboratory, Michigan State University, East Lansing, MI 48824 USA

Abstract

Multinucleon-transfer reactions are used to measure the ground state masses of light nuclei far from beta stability. Techniques for particle identification and Q-value measurements in a magnetic spectrograph are discussed, and the results of the experiments are compared to various theoretical models.

1. Introduction

Transfer reactions can be used to measure nuclear masses with high precision, and the techniques which have evolved to make these measurements in a magnetic spectrograph are now being applied to nuclei far from beta stability in a number of laboratories. Besides providing a means of Q-value determination, the spectrograph has proven to be extremely valuable in the particle detection aspects of the problem. Of equal importance has been the advent of cyclotrons with well-defined, precise, high-energy beams. The cyclotron-spectrograph combination is capable of measuring masses to an accuracy in the kilovolt range in spite of the high particle energies involved which are in the range of 25-100 MeV. In this paper we will first discuss the techniques for particle identification and Q-value measurements. It will be evident that most of the physical effects we are discussing would not be visible if the accuracy of the measurements were not so high.

2. Method

A list of the transfer reactions which have been involved in studies of nuclei far from stability is given in Table I. The

TABLE I.--List of transfer reactions used to study nuclei far from beta stability.

ΔA	REACTION	ΔN	ΔP	ΔT_z	Q-values MeV	$\sim d\sigma/d\Omega^*$ $\mu\text{b/sr}$
3	(p, ^4He)	2	1	1/2	-7	50
	(^3He , ^6Li)	1	2	-1/2	-11	50
	(^3He , ^6He)	3	0	3/2	-27	1
4	(^3He , ^7Be)	2	2	0	-8	10
	(^3He , ^7Li)	3	1	1	-21	2
	(^4He , ^8He)	4	0	2	-60	0.01
5	(^3He , ^8B)	2	3	-1/2	-20	0.2
	(^3He , ^8Li)	4	1	3/2	-33	0.1
	(p, ^6He)	4	1	3/2	-37	0.1
	(^3He , ^8He)	5	0	5/2	-52	0.0002
6	(^3He , ^9Li)	5	1	2	-51	0.005
	(^3He , ^9C)	2	4	-1	-30	<0.002

*75 MeV ^3He
45 MeV p

cross sections and Q-values given are typical ones for the particular reaction. The cross sections show a strong fall off with number of transferred particles and with transferred T_z . Not surprisingly, therefore, the farther from stability one

wants to go, the lower the cross section. Extreme limits of nuclear stability can be reached by these reactions provided that nature has presented the appropriate targets. For example the two extremes of knowledge of the Cl isotopes, ^{31}Cl and ^{43}Cl , were both reached by five nucleon transfer reactions: $^{36}\text{Ar}(^3\text{He}, ^8\text{Li})^{31}\text{Cl}$ and $^{48}\text{Ca}(^3\text{He}, ^8\text{B})^{43}\text{Cl}$. The cross-sections for these reactions were approximately 10-25 nanobarns/sr. In all cases in which the cross section exceeded a few nanobarn/sr, a reasonable accurate mass has been obtained (<60 keV). The technique described here is responsible for the most accurate mass determinations of approximately 25 nuclei far from stability ranging from ^8C to ^{55}Ni and the first observation of about 15 of them.

In Fig. 1 we give an unusually complete view of the experimental apparatus used at Michigan State University. The maximum energy beams from the cyclotron are 76 MeV for ^3He 's and 48 MeV for protons, and typical beam currents are 1 to 4 μA . At these currents the energy resolution of the cyclotron-spectrograph combination is less than the target thickness energy spread. The best energy resolution that has been obtained is 25 keV. In this case the beam, target and detector contributed about equally to the resolution. Good resolution is very important in both accurate Q-value measurements and in separating the peaks of interest from the background.

The detector is a triple telescope consisting of two wire counters and a plastic scintillator. The front wire counter measures the energy loss, $\Delta E'$, redundantly with the energy loss in the second counter, ΔE . In the present setup, a single channel analyser which is set on the $\Delta E'$ of the group of interest is one of the gate requirements for the other signals to reach the computer. By going from four to six ADC's we are planning to add the position information from this wire to the events recorded on tape. At present only the second wire gives position information (by resistive charge division). The spatial resolution is about 0.5 mm and usually contributes negligibly to the overall resolution. The principle of operation of a charge-division position sensitive detector is shown in Fig. 2. The computer constructs the energy loss by adding the signals to get ΔE and then taking the division $E_1/\Delta E$. Time of flight relative to the rf structure of the beam is also recorded as is the light output from the scintillator. This light signal is rather poor in quality and can not distinguish well between particle types. The plastic scintillator has another defect in that it is very gamma sensitive; keeping the raw counting rate in each detector to a minimum is crucial for suppressing background. For a plastic scintillator minimum volume is therefore important. We use 0.2 mm thick Pilot B scintillator, which is so thin that

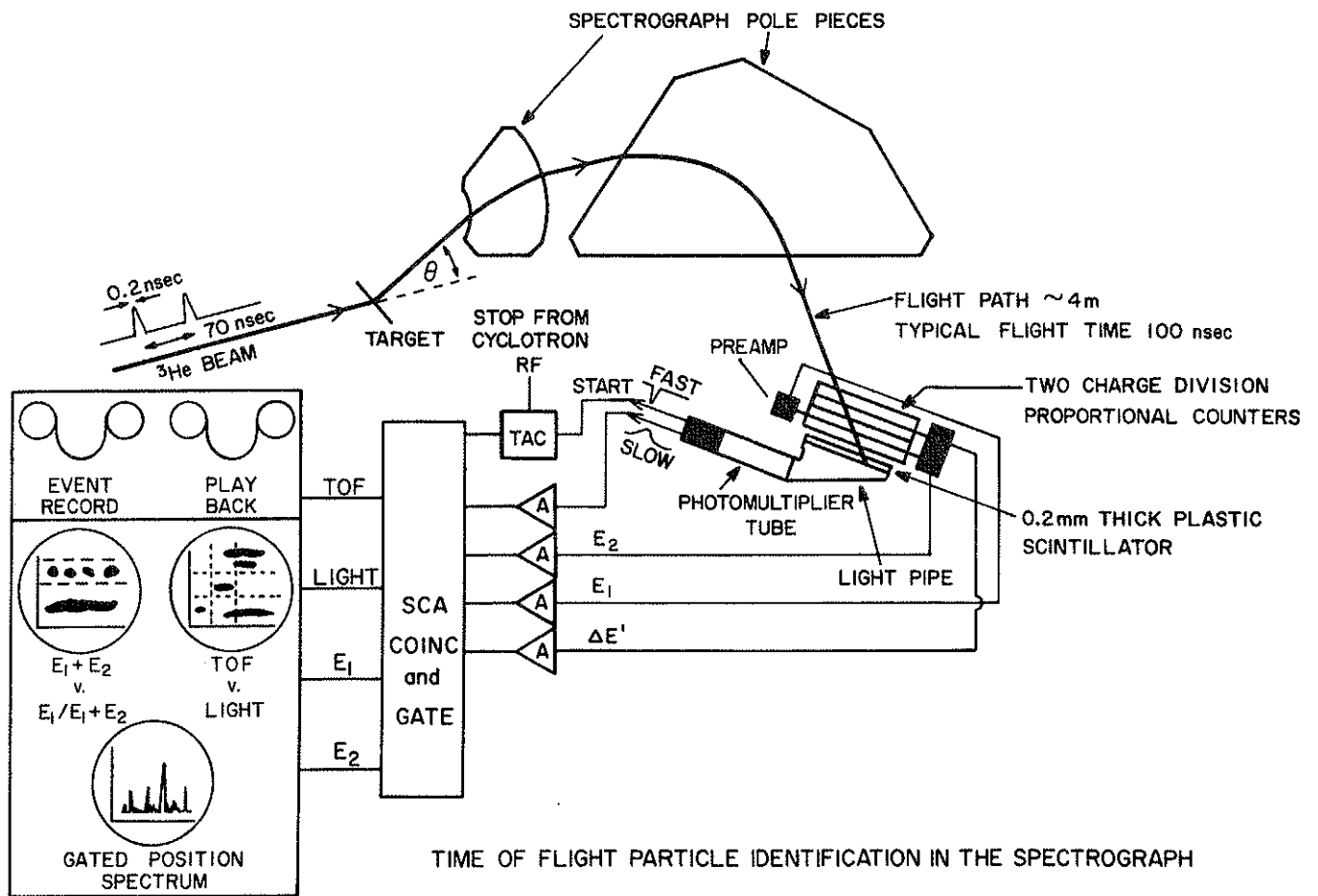


FIG. 1.--Schematic representation of experimental arrangement.

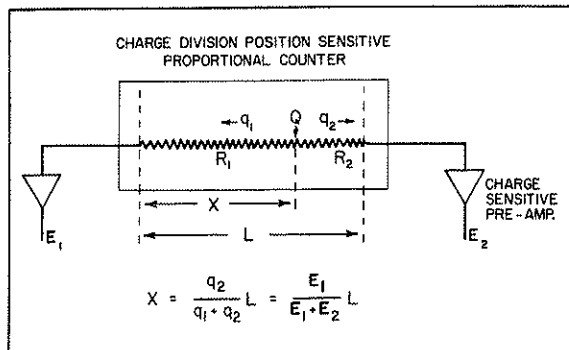


FIG. 2.--Principle of operation of a charge-division proportional counter.

the particles of interest actually pass through it. Ions give little light at the end of their range and therefore little signal is lost and the gamma count rate is minimized. A good solution to the gamma-ray and poor resolution problem of the plastic scintillator is to replace it with a silicon detector. The problem here is limited length, but a recent run with a 50 cm long surface barrier detector gave a very low background level of 50 picobarns/sr-MeV in a search for the $^{27}\text{Al}(^3\text{He}, ^8\text{He})^{22}\text{Al}$ reaction.

Figure 3 gives one of the displays

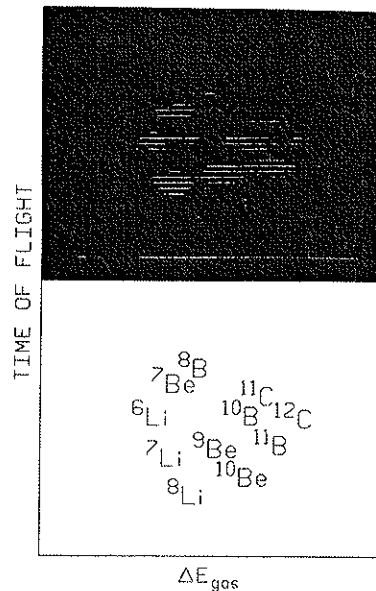


FIG. 3.--A display of ΔE versus time-of-flight. The particles are produced by a 74 MeV ^3He beam on a ^{12}C target.

that may be observed from the computer, ΔE , energy loss in the gas, versus time-of-flight. Any combination of the four input signals can be displayed gated by another.

The events are stored on tape and either live data or a previous tape can be analyzed into spectra like that seen in Fig. 4, which is from the $^{24}\text{Mg}(^3\text{He},^8\text{Li})^{19}\text{Na}$ reaction. Playback of the tape is not always required since the gates can be set effectively from a small amount of initial data. Sometimes

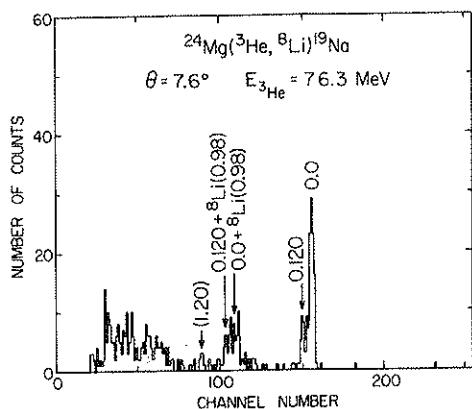


FIG. 4.--Spectrum of the $^{24}\text{Mg}(^3\text{He}, ^8\text{Li})^{19}\text{Na}$ reaction.

it is very useful for the cleaning up of data as is shown in Fig. 5. The lower spectra is of the $^{50}\text{Cr}(^3\text{He}, ^6\text{He})$ reaction taken on-line. The improved version is the upper spectrum in the figure. The lower level on the energy loss requirement was raised during the playback, and as a result ambiguities concerning the ground state region were eliminated. The background events which were eliminated are due to the simultaneous arrival of an alpha and a triton.

The techniques for determining the Q-value from the gated position spectrum have been described previously.¹ The method is a comparative one with known reactions placed on the same focal plane position by small changes of field. Reactions with similar rigidity outgoing particles but different Q-values, e.g. $(^3\text{He}, ^4\text{He})$ and $(^3\text{He}, ^6\text{He})$, are very useful for beam energy determination; a technique known as momentum matching.² A useful trick to eliminate the effect of gains and zero levels when comparing different particle types is to adjust the gas gain to give each particle type the same energy loss signal in the wire counter. Calibration reactions with detected particle and Q-value similar to that of the reaction of interest are used whenever possible. An example is the $(^3\text{He}, ^6\text{He})$ comparisons shown in Fig. 6. The experiment was a mass measurement of ^{37}Ca using ^{21}Mg and ^{55}Ni as calibrations. Ideally one wants one calibration above and one below the primary reaction in rigidity. This allows an interpolation between two fields, and knowledge of magnetic field integral versus NMR setting becomes unimportant.

The error obtained in a particular experiment is usually determined by a number of factors. A typical case³ is shown in Table II. One can see that a number of improvements would have to be made

TABLE II.--Error analysis for a ^{19}Na mass determination.

$^{24}\text{Mg}(^3\text{He}, ^8\text{Li})^{19}\text{Na}$ vs $^{24}\text{Mg}(^3\text{He}, ^7\text{Li})^{20}\text{Na}$		
PARAMETER	UNCERTAINTY	EFFECT ON ^{19}Na MASS (keV)
E_{in} (ABSOLUTE)	30 keV	6.6
" (FLUCTUATION)	16 keV	8.0
θ	0.15°	3.0
$\sigma(\theta)$	~0.25°	5.0
CENTROIDS	0.3 CHANNELS	6.3
^{20}Na MASS	6 keV	4.7
ΔE TARGET	~10%	1.0<
B SCALING	—	1.0<
B REPRODUCIBILITY	1/20,000	4.0
COUNTER LINEARITY	—	1.0<
		15.0

besides collecting more counts. The beam energy fluctuation problem could perhaps be eliminated by constant monitoring of the elastic line, but this would only be advantageous if the absolute error could also be improved. A 30 keV error for a ^3He beam energy of 76 MeV is at the limit of the momentum matching method.

Fig. 7 and 8 shows two spectra from the $^{40}\text{Ca}(^3\text{He}, ^8\text{Li})$ reaction⁴ to illustrate the advantage of good resolution. The two runs were taken for the same charge and spectrograph solid angle, but in the second a much thinner target was used. Since the resolution was limited by target thickness in this case, the second ^{35}K peak has the same height but much fewer counts. It is actually a much better measure of the mass since the centroid error is linear with the width but decreases only with the square root of the number of counts. In this case one can also be much surer of the absence of shifts due to background.

3. Results

It is not possible to list here all of the masses which have been measured by these techniques. In any case most have become part of the most recent tables. Instead we will discuss their significance in terms of three general mass headings 1) the isobaric multiplet mass equation 2) Coulomb energies in the $f_{7/2}$ shell and 3) comparison to various methods for mass extrapolation.

3.1 Isobaric Multiplets

The isobaric multiplet mass equation has been reviewed in several publications.⁵ The basic idea is that a state of isospin T is one member of a $2T+1$ multiplet, which would be degenerate in the absence of charge dependent effects. Wigner⁶ showed that, in first order perturbation theory, charge dependent two-body forces can at most produce a quadratic dependence of the mass on the z-projection of isospin, T_z .

$$M(T_z) = a + bT_z + cT_z^2$$

To check this result one needs a multiplet with $T > 3/2$. This is where nuclei far from stability enter the picture. The $T_z = -3/2$ nucleus is in every case three or

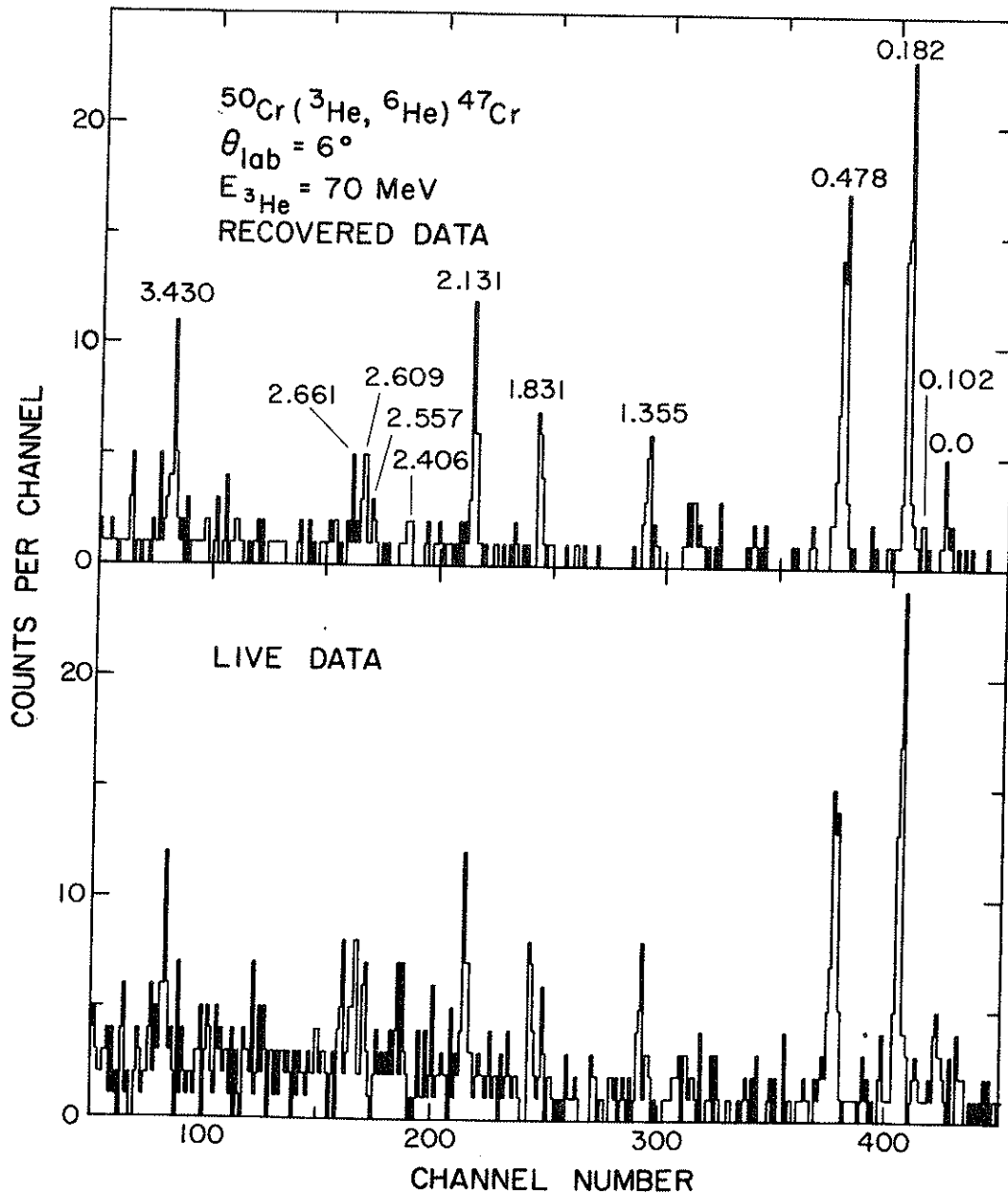


FIG. 5.--Comparison of live to recovered data from the $^{50}\text{Cr} (^3\text{He}, ^6\text{He}) ^{47}\text{Cr}$ reaction.

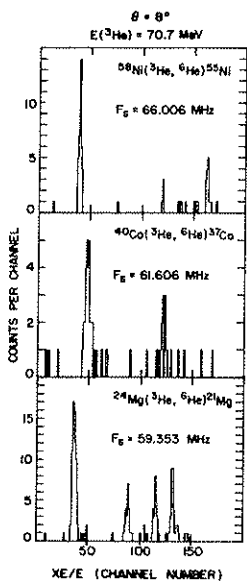


FIG. 6.--Spectra taken for a mass measurement of ^{37}Ca .

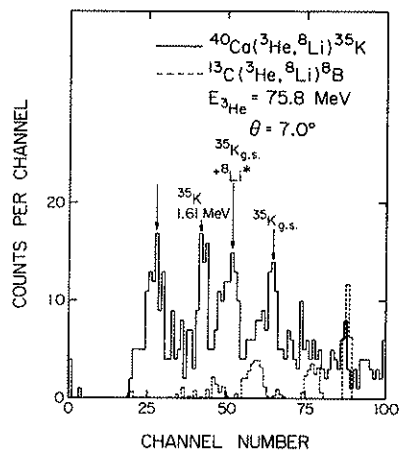


FIG. 7.--Spectrum of the $^{40}\text{Ca} (^3\text{He}, ^8\text{Li})$ reaction with a $300 \mu\text{g}/\text{cm}^2$ target.

more nuclei from stability. By means of the (${}^3\text{He}, {}^6\text{He}$) and (${}^3\text{He}, {}^8\text{Li}$) reactions we have now measured all the $T_z = -3/2$ masses from ${}^9\text{C}$ to ${}^{37}\text{Ca}$ with the two exceptions of ${}^{15}\text{F}$ and ${}^{27}\text{P}$. These two are being worked on but are extremely difficult because of target problems. The (${}^4\text{He}, {}^8\text{He}$) or perhaps some heavy ion reactions may prove superior for these nuclei and in fact for the continuing extension of this work towards the line of proton or two-proton emission. Not all of the mass measurements of $T_z = -3/2$ nuclei have resulted in complete mass quartets. Often one of the other members is difficult to observe experimentally. The $A=19$ ground state quartet has been completed recently⁷ by observing the lowest $T=3/2$ state in ${}^{19}\text{Ne}$ by means of the ${}^{21}\text{Ne}(p, t){}^{19}\text{Ne}$ reaction. The $A=35$ quartet has not been completed⁴ because of the difficulty of observing the $T=3/2$ state in ${}^{35}\text{Ar}$. A known state of the same spin but $T=1/2$ lies right at the predicted energy. Another recently completed quartet is the $A=31$ ground state. We have recently employed the ${}^{36}\text{Ar}({}^3\text{He}, {}^8\text{Li})$ reaction to measure the mass excess of ${}^{31}\text{Cl}$ to be -7.07 ± 0.05 MeV [$Q = -29.176$].

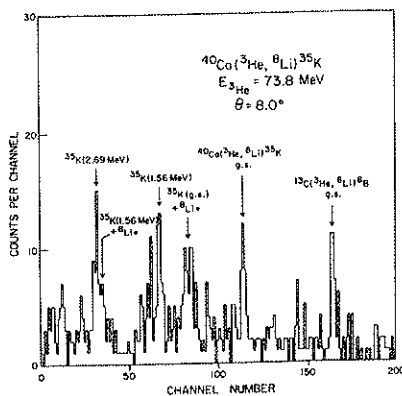


FIG. 8.--Spectrum of the ${}^{40}\text{Ca}({}^3\text{He}, {}^8\text{Li})$ reaction with a $170 \mu\text{g}/\text{cm}^2$ target.

Fig. 9 summarizes the current situation on mass quartets by displaying d , the coefficient of a T_z^3 term needed to fit the data exactly. The agreement is astonishing over a wide range of A and including both ground and excited states. The significance of this appears to be that the wave function of the members of the multiplet remains essentially unchanged as the T_z is changed--even if the most proton rich nucleus becomes much less bound or even unbound, e.g. ${}^{19}\text{Na}$.

The sole strong disagreement with the predictions of the multiplet equation is the ground state $A=9$ quartet.⁸ There are several remarks that should be made about this. First it is the most accurately measured quartet by far, the $T_z = \pm 1/2$ members having been measured to about 1 keV and the $T_z = \pm 3/2$ members to about 3-4 keV. Secondly, it is the lightest quartet with all members bound. The ${}^9\text{C}$ mass was measured to an accuracy of 4 keV with the ${}^7\text{Be}({}^3\text{He}, n)$ reaction.⁹ We have attempted to verify this result with the ${}^{12}\text{C}({}^3\text{He}, {}^6\text{He}){}^9\text{C}$ reaction and the result, while agreeing with the (${}^3\text{He}, n$) measurement, would move the d -coefficient closer to zero. The experi-

mental error in this case is about 8 keV so it has a negligible effect when averaged with the (${}^3\text{He}, n$) number. Surprisingly the first excited state $A=9$ quartet, which contains unbound levels, is closer to a quadratic multiplet equation as can be seen in Table III.

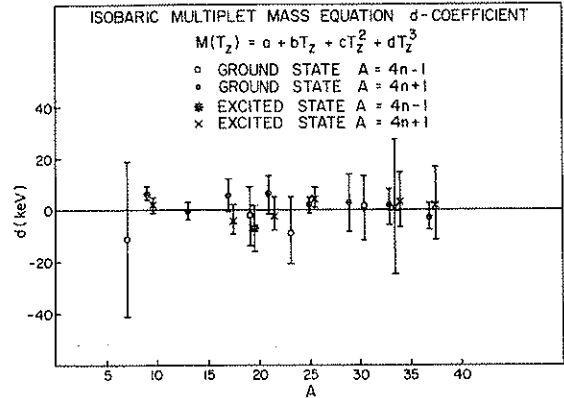


FIG. 9.-- d -coefficient of the isobaric multiplet equation versus A . Excited states are displaced slightly to the right of the appropriate A .

TABLE III.--The two $A=9$ mass quartets.

A = 9 QUARTETS		
	d (keV)	χ^2
g.s.	$\equiv 0$	14
	5.8 ± 1.5	-
1 st exc.	$\equiv 0$	0.6
	2.3 ± 2.9	-

Mass quintets constitute a much more severe test of the isobaric multiplet equation than do quartets. The first one, $A=8$, was completed about a year ago,¹⁰ but only recently have accurate mass measurements been available for all five members. These five measurements were all made by transfer reactions in a magnetic spectrograph using techniques of the type described above. The agreement here is even more amazing than the many quartets. Table IV summarizes the situation for the mass quintets. The significance of an e -coefficient in $A=8$ is related to isospin mixing in ${}^8\text{Be}$ as is discussed in Ref. 11. The $A=20$ quintet has four members known. Both $A=8$ and $A=20$ $T_z = -2$ members were measured most accurately at Texas A&M with the (${}^4\text{He}, {}^8\text{He}$) reaction,^{12, 13} A spectrum of this reaction leading to ${}^{20}\text{Mg}$ is shown in Fig. 10.

3.2 Coulomb Energies in the $f_{7/2}$ Shell

The eight $T_z = -1/2$ nuclei in the $f_{7/2}$ shell now have accurate mass measurements. The mirror Coulomb energies associated with these masses are plotted in Fig. 11.

TABLE IV.--Summary of Mass Quintet Coefficients (keV).

A	d	e	χ^2
8	0	0	6.6
8	6.0±2.6	0	1.2
8	0	4.0±1.9	2.2
8	4.4±3.0	2.4±2.2	--
20	0	0	1.35
20	2.3±2.0	0	--

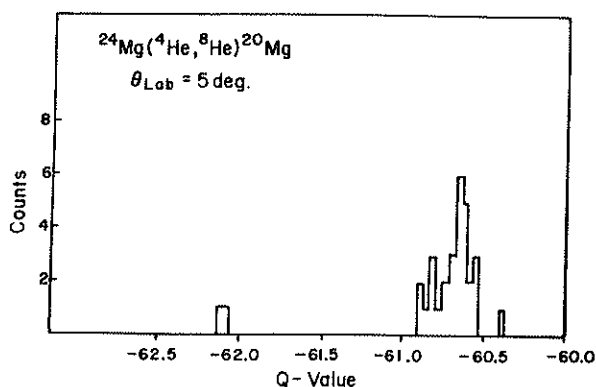


FIG. 10.--Spectrum from the mass measurement of ^{20}Mg by Tribble, et al.¹³

The Coulomb energies have been divided by the Z of the neutron-rich member, and one can see an alternation due to Coulomb pairing, which would not be visible if the errors on the masses were not below 30 keV. The mass 49 point has recently moved right onto the line due to a new mass measurement of the non-exotic nucleus, ^{49}Cr , at Notre Dame.¹⁴ The Coulomb pairing occurs because more energy is lost when a paired proton is converted to a neutron than when an unpaired one is. The shell model calculations of Chung and Wildenthal¹⁵ shown as a solid line reflect this effect very nicely. For comparison the same effect is shown for the $d_{5/2}$ shell where it is much more marked.

Coulomb displacement energies of hole states in the $A=4n+1$ mirror nuclei can be described by a simple model,¹⁶ but first these states have to be identified. This was done by comparison to the known spins in the mirror nucleus and also by means of angular distributions which were compared to the angular distributions from the $^{42}\text{Ca}(^3\text{He}, ^6\text{He})$ reaction as is shown in Fig. 12. The Coulomb displacement energy of a $3/2^+$ hole state in the $f_{7/2}$ shell is related to that in $A=39$ by the relations

$$E_c(A) = E_c(39) + C \frac{A-39}{2}$$

where C is a constant.

Thus a plot of $E_c(A)$ versus A should be a straight line. That this is nearly the case is shown in Fig. 13. The $A=39$ energy should be corrected by 125 keV for its much larger binding than the other three nuclei. The slope corresponds to $C=300$ keV which is in good agreement with a previous determination by Sherr and Bertsch of essentially the same physical quantity, namely the Coulomb interaction between an $f_{7/2}$ particle and a $d_{3/2}$ hole.

3.3 Mass Extrapolations

Only the symmetric Garvey-Kelson¹² mass formula (shown in Fig. 14) can be used to cross the $N=Z$ line. The masses of a series of $T_z=-1/2$ nuclei must be known, however. This is what has limited extrapolations mainly to $N>Z$ nuclei. By measuring the $T_z=-1/2$ nuclei up to ^{55}Ni we have been able to extend the relation to $Z>N$ nuclei up to the Ni. The resulting predictions, which were made using the symmetric relation are given in Table V. One can see that it will be a long time before the limits of stability are reached for light proton-rich nuclei or the interesting 2-proton emitters can be studied.

Recently we have begun to apply the same techniques to neutron-rich nuclei. Fig. 15 gives spectra from the $(^3\text{He}, ^8\text{B})$ reaction on ^{64}Ni and ^{27}Al . The latter provided a calibration for the mass measurement of ^{59}Mn which is summarized in Table VI. In Fig. 16 we show the $^{48}\text{Ca}(^3\text{He}, ^8\text{B})^{43}\text{Cl}$ reaction, which unfortunately has a Q -value so negative that the ^{43}Cl peak falls in the region of light contaminants. The ^{43}Cl results are also summarized in Table VI, which also gives a comparison of the two neutron-rich nuclear masses to various theoretical models. These measurements of nuclei far from stability are more accurate than those obtained by other methods and therefore serve as good points to tie the various extrapolations down and also as good calibration nuclei for the other methods.

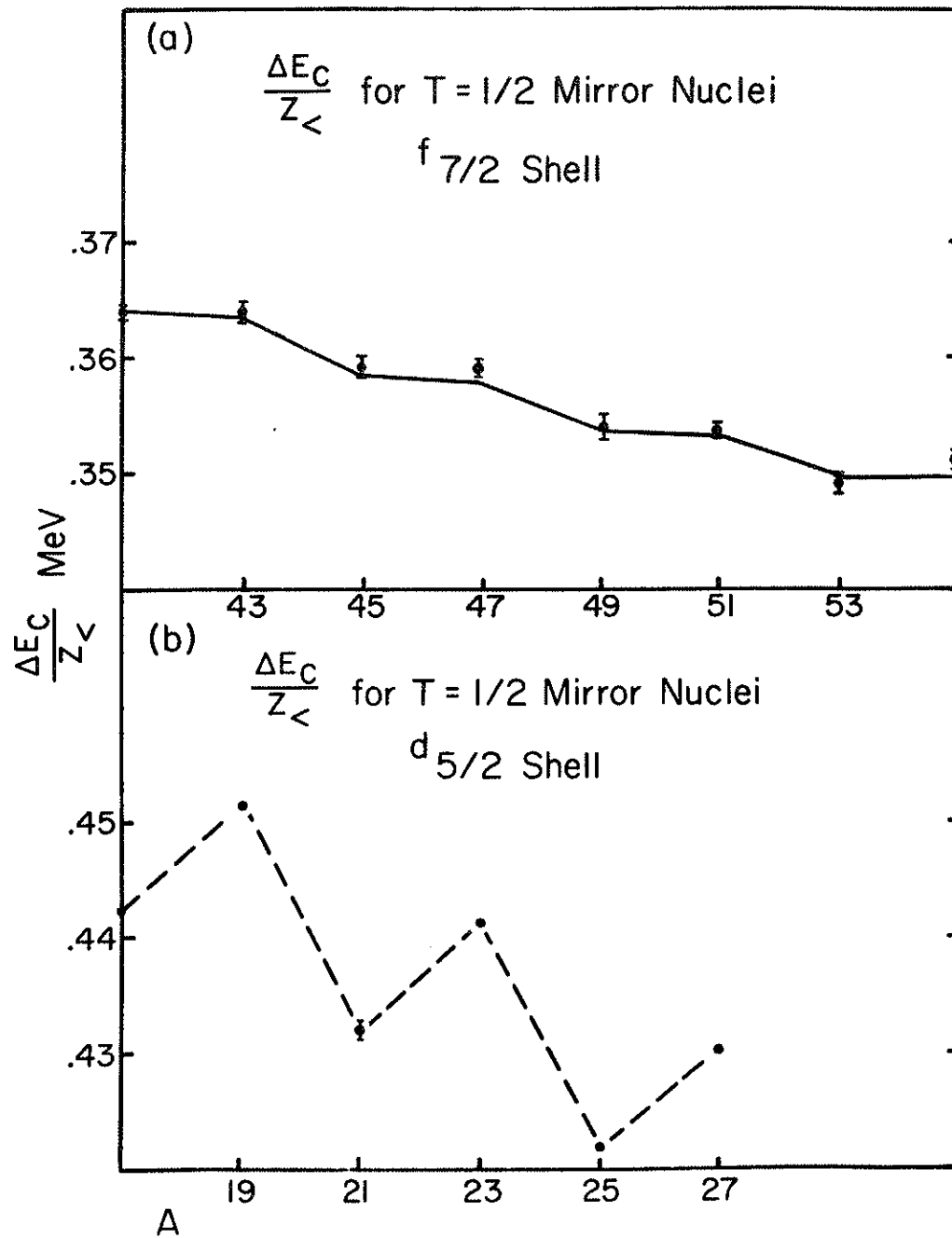


FIG. 11.--Coulomb displacement energies in the $f_{7/2}$ and $d_{5/2}$ shells.

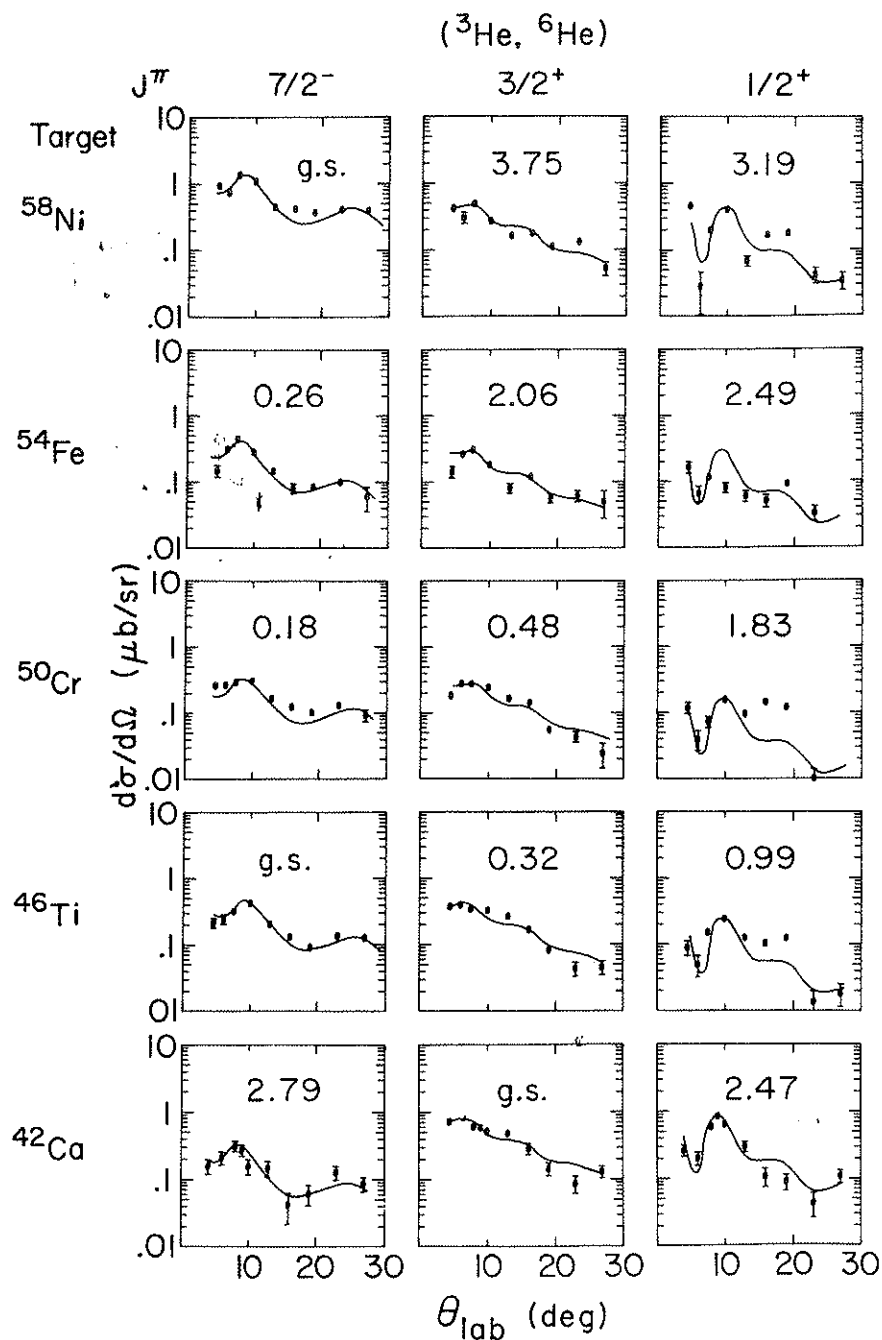


FIG. 12.--Angular distributions for $7/2^-$, $3/2^+$ and $1/2^+$ states excited by the (${}^3\text{He}, {}^6\text{He}$) reaction.

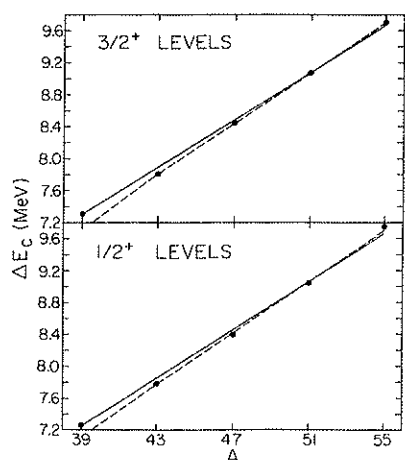


FIG. 13.--Coulomb displacement energy versus A for $3/2^+$ and $1/2^+$ states in ${}^{4n+1}$ mirror nuclei in the $f_{7/2}$ shell.

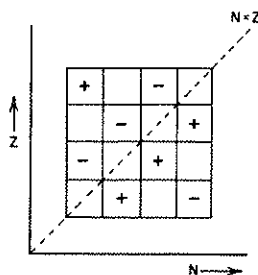


FIG. 14.--The Garvey-Kelson symmetric mass relation.

TABLE V.--Predicted mass excess using the symmetric Garvey-Kelson mass relation.^a

Nucleus	Mass excess (MeV)	Separation energy ^b (MeV)	
		One proton	Two protons
$T_Z = -1$			
⁴⁴ V	-23.83	1.81	6.31
⁴⁶ Cr ^c	-29.56	5.02	6.64
⁴⁸ Mn	-29.31	2.03	6.81
⁵⁰ Fe	-34.50	4.13	6.22
⁵² Co	-34.38	1.48	6.34
⁵⁴ Ni	-39.27	3.92	5.53
$T_Z = -\frac{3}{2}$			
⁴³ V	-17.92	0.10	3.87
⁴⁵ Cr	-19.64	3.14	4.95
⁴⁷ Mn	-22.65	0.32	5.34
⁴⁹ Fe	-24.76	2.76	4.79
⁵¹ Co	-27.40	0.19	4.32
⁵³ Ni	-29.66	2.59	4.07
$T_Z = -2$			
⁴² V	- 8.02	-0.37	2.09
⁴⁴ Cr	-13.54	2.96	3.06
⁴⁶ Mn	-12.62	0.22	3.36
⁴⁸ Fe	-18.17	2.82	3.14
⁵⁰ Co	-17.73	0.26	3.02
⁵² Ni	-22.68	2.58	2.77
$T_Z = -\frac{5}{2}$			
⁴¹ V	0.08	-1.81	0.43
⁴³ Cr	- 2.14	1.45	1.08
⁴⁵ Mn	- 5.17	-1.14	1.82
⁴⁷ Fe	- 7.15	1.84	2.06
⁴⁹ Co	- 9.95	-0.93	1.89
⁵¹ Ni	-12.02	1.59	1.85
$T_Z = -3$			
⁴² Cr	6.17	1.25	-0.56
⁴⁴ Mn	6.35	-1.26	0.19
⁴⁶ Fe	0.53	1.60	0.46
⁴⁸ Co	0.97	-0.84	1.00
⁵⁰ Ni	- 4.13	1.49	0.56
$T_Z = -\frac{7}{2}$			
⁴⁵ Fe	13.58	0.08	-1.18
⁴⁹ Ni	7.61	0.67	-0.17
$T_Z = -4$			
⁴⁸ Ni	16.43	0.50	-1.31

^aMasses used in the relation are the present experimental results, Mass 71 mass values of A.H. Wapstra and N.B. Gove, Nucl. Data A9, 267(1971), for the ⁵⁵Co mass excess is -54.0275±0.0022 MeV from P.L. Jolivette, *et al.* Phys. Rev. C10,2449(1974) and for the mass excess of ⁴⁹Cr is -45.327±0.0029 MeV from P.L. Jolivette, *et al.* private communication and Phys. Rev. C13,439(1976).

^bNegative binding energy indicates nucleus unbound to particle emission.

^cExperimental mass excess is -29.46±0.03 J. Zioni, *et al.*, Nucl. Phys. A181,465(1972).

TABLE VI.--Summary of Mass Measurements on ^{59}Mn and ^{43}Cl .

Final nucleus reached by the ($^3\text{He}, ^8\text{B}$) reaction.	^{59}Mn	^{43}Cl	
Q-value in MeV	-19.61 ± 0.03	-29.07 ± 0.06	
$d\sigma/d\Omega$ at 90° in $\mu\text{b/sr}$	0.05 ± 0.01	0.02 ± 0.01	
experimental mass excess	-55.49 ± 0.03	-23.14 ± 0.06	Ref.
predicted mass excess			
Garvey-Kelson (69)	-55.75	-23.78	A
Garvey-Kelson (75)	-56.01	-23.64	B
Garvey-Kelson (76)	-55.79	-23.38	C
Modified G-K	-56.35	-23.61	B
Liran-Zeldes	-56.01	-23.00	D

- A. G.T. Garvey, *et al.*, Rev. Mod. Phys. **41**, 511(1969).
 B. N.A. Jelley, *et al.*, Phys. Rev. **C11**, 2049(1975) and C.N. Davids, to be published.
 C. W. Gerace, private communication
 D. S. Liran and N. Zeldes, Institut für Kernphysik der Technischen Hochschule, Darmstadt, IKDA75114, unpublished.

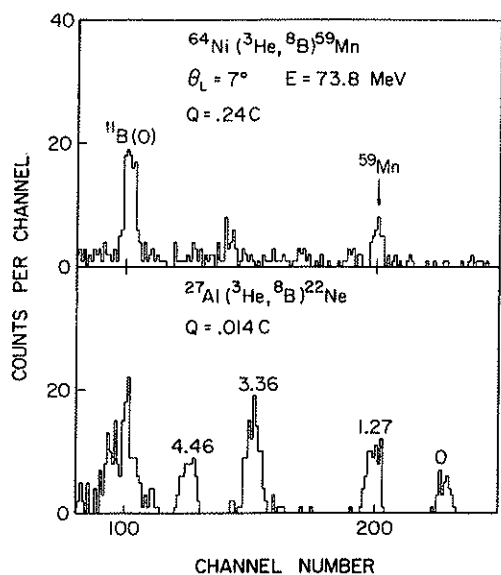


FIG. 15.--Spectra from the mass measurement of ^{59}Mn . The calibration reaction $^{27}\text{Al}(^3\text{He}, ^8\text{B})^{22}\text{Ne}$ and the $^{64}\text{Ni}(^3\text{He}, ^8\text{B})^{59}\text{Mn}$ run at the same field.

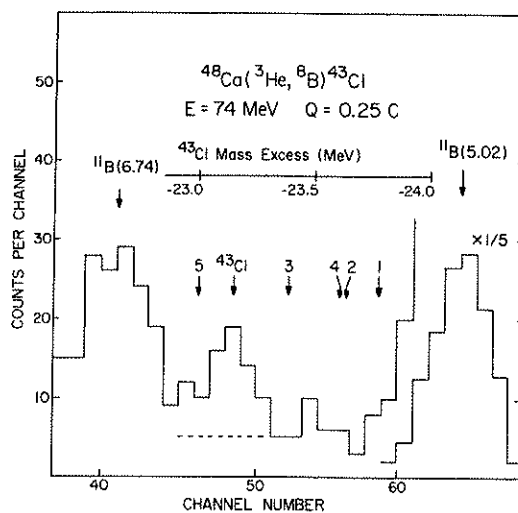


FIG. 16.--Spectrum from the mass measurement of ^{43}Cl . Predictions 1-5 refer to Garvey-Kelson(69), Garvey-Kelson(75), Garvey-Kelson(76), Jelley, *et al.* and Livran and Zeldes as given in Table VI above.

*Work supported by U.S. National Science Foundation.

REFERENCES

1. J.A. Nolen, Jr., G. Hamilton, E. Kashy and I.D. Proctor, Nucl. Inst. and Meth. 115,189(1974).
2. E. Kashy, W. Benenson and D. Mueller Atomic Masses and Fundamental Constants J.H. Sanders and A.H. Wapstra, eds. Plenum Press, New York-London 1976, p.140.
3. W. Benenson, A. Guichard, E. Kashy, D. Mueller, H. Nann and L.W. Robinson, Phys. Letters 58B,46(1975).
4. W. Benenson, A. Guichard, E. Kashy, D. Mueller and H. Nann, Phys. Rev. C13,1479(1976).
5. W. Benenson and E. Kashy, Atomic Masses and Fundamental Constants J.H. Sanders and A.H. Wapstra, eds. Plenum Press, New York-London 1976, p.154 and references therein.
6. E.P. Wigner, Proceedings of the Robert A. Welch Foundation Conference on Chemical Research 1957, Edited by W.D. Millikan.
7. H. Nann and H.T. Fortune, private communication.
8. E. Kashy, W. Benenson and J.A. Nolen, Jr., Phys. Rev. C9,2102(1974).
9. J.M. Mosher, R.W. Kavanagh and T. Tombrello, Phys. Rev. C3,438(1971).
10. R.G.H. Robertson, W.S. Chien and D.P. Goosman, Phys. Rev. Lett. 34, 33(1975).
11. R.G.H. Robertson, W. Benenson, E. Kashy and D. Mueller, Phys. Rev. C13, 1018(1976).
12. R.E. Tribble, R.A. Kenefick and R.L. Spross, Phys. Rev. C13,50(1976).
13. R.E. Tribble, J.D. Cossaint, and R.A. Kenefick, (to be published).
14. P.L. Jolivette, J.D. Goss, J.A. Bieszk, R.D. Hichwa and C.P. Browne, Phys. Rev. C13,439(1976).
15. W. Chung and B.H. Wildenthal (to be published).
16. R. Sherr and G. Bertsch, Phys. Rev. C12,1671(1975).